NJC

New Journal of Chemistry

An international journal of the chemical sciences

www.rsc.org/njc

Volume 32 | Number 12 | December 2008 | Pages 2053–2304

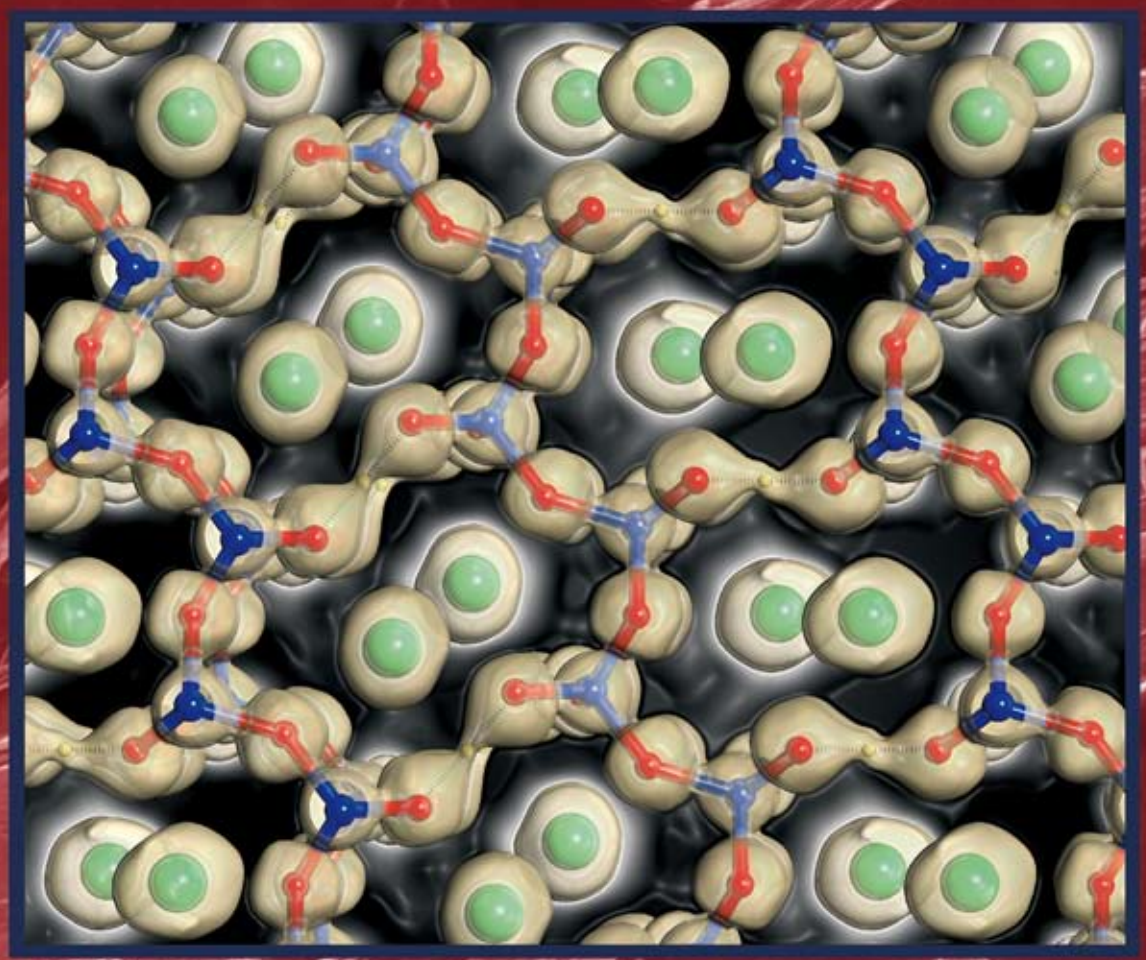

ISSN 1144-0546

RSC Publishing

CNRS CENTRE NATIONAL DE LA RECHERCHE SCIENTIFIQUE

PAPER

Takuji Ikeda *et al.*

Pseudo-micropores formed by one-dimensional framework with hydrogen bonding in $CsHSi_2O_5$ observed by synchrotron powder diffraction and solid-state MAS NMR

Pseudo-micropores formed by one-dimensional framework with hydrogen bonding in $CsHSi_2O_5$ observed by synchrotron powder diffraction and solid-state MAS NMR

Takuji Ikeda,*[a] Toshikazu Nishide,[b] Hiroko Nakajima,[b] Akiko Kawai,[a] Yoshimichi Kiyozumi,[a] Tetsuya Kodaira[c] and Fujio Mizukami[a]

Received (in Durham, UK) 9th May 2008, Accepted 4th July 2008
First published as an Advance Article on the web 5th September 2008
DOI: 10.1039/b807879c

One-dimensional fibrous low dimensional caesium silicate, LDS-1, was synthesized by performing solid-state reactions with dry gels of silica containing tetrabutylammonium and caesium cations. We report the detailed crystal structure of LDS-1 comprising alternating alignments of zigzagged frameworks with four-membered rings and strong hydrogen bonds between adjacent terminal silanols; this structure is very similar to that of $CsHSi_2O_5$, whereas their crystal symmetries are different. The chain-like frameworks with a Q^3 ($(SiO)_3SiOH$) local structure form an elliptical topology with pseudo-micropores by strong hydrogen bonding. The hydrogen bonding was clearly observed in the electron density distributions analyzed by the maximum entropy method using high-resolution synchrotron powder diffraction data. Solid-state MAS NMR spectroscopy also exhibits strong hydrogen bonding between adjacent oxygen atoms, as indicated by an atomic distance of d(O–O) $\approx$ 2.45 Å. The elliptical spaces hold large caesium cations.

1. Introduction

Layered and porous crystalline silicates such as clays and zeolites[1] are widely used as catalysts, adsorbents, desiccants, detergents, sensors, and so on, and their structural design is very important due to the close relationship between structure and performance. Linear or layered silicates are the fundamental structures for various crystalline silicates and are potential precursors and building blocks for useful industrial crystalline silicates. Solid-state transformations of layered silicates to microporous materials have been investigated[2–7] and found to form porous crystals much faster than the corresponding conventional hydrothermal syntheses. Designing linear silicate chains is, therefore, very attractive since linear frameworks are easily converted into two- or three-dimensional networks by the dehydration condensation of terminal silanols.

A large number of infinite linear silicates are known and examples of linear silicates that have been crystallographically identified.[8–17] However, such linear silicates that include only a caesium (Cs) cation have been barely reported. In this study, we report a low-dimensional caesium silicate (abbreviated as LDS-1),[18] which is a very similar polymorph of $CsHSi_2O_5$ reported by Dörsam *et al.*[19] LDS-1 was obtained under solid-state reaction conditions. The crystal structure of $CsHSi_2O_5$ comprises alternating alignments of zigzagged silica frameworks, and the Cs cations are stabilized in the elliptical spaces formed by the chain-like framework. It was revealed that adjacent frameworks are connected by strong hydrogen bonding, *i.e.*, one proton is shared between neighboring terminal silanol oxygen atoms such as the $(SiO)_3SiO–H\cdots OSi(SiO)_3$ configuration. However, the hydrogen bonding of silanols is usually difficult to observe directly by X-ray diffraction, although its behavior is very interesting and important for understanding the structural stability of silicates. More recently, several examples of topotactic conversion from layered silicates to zeolites were reported as novel zeolite synthesis methods.[20–23] In these works, strong hydrogen bonding plays an important role for bridging neighboring frameworks by the dehydration condensation of terminal silanol groups.

In this work, obvious electron density distribution is analyzed by means of the maximum entropy method (MEM)[24] using synchrotron powder diffraction data in order to crystallographically elucidate strong hydrogen bonding in LDS-1. Thermal stability and crystal morphology of LDS-1 were characterized. We also investigated the local environments for Si, Cs and H atoms by solid-state magic-angle spinning nuclear magnetic resonance (MAS NMR).

2. Experimental

2.1 Synthesis

We initially discovered the LDS series while examining the effect of alkali-metal cations on the solid-state synthesis[25] of

[a] *Research Center for Compact Chemical Process, National Institute of Advanced Industrial Science and Technology (AIST), 4-2-1, Nigatake, Miyagino-ku, Sendai, 983-8551, Japan. E-mail: takuji-ikeda@aist.go.jp; Fax: +81-22-237-5217; Tel: +81-22-237-3016*
[b] *Department of Materials Chemistry and Engineering, College of Engineering, Nihon University, Tamura, Koriyama, Fukushima, 963-8642, Japan. E-mail: nishide@ce.nihon-u.ac.jp; Fax: +81-24-956-8862; Tel: +81-24-956-8882*
[c] *Research Center for Compact Chemical Process, National Institute of Advanced Industrial Science and Technology (AIST), 1-1-1, AIST Tsukuba Central 5, Tsukuba, Ibaraki, 305-8565, Japan. E-mail: kodaira-t@aist.go.jp; Fax: +81-29-861-4631; Tel: +81-29-861-4631*

zeolites from silica gels. LDS tended to form when the cations had a relatively large ionic size (*e.g.*, Cs^+ and Rb^+), and the content or the ratio of the cations to Si in the synthesis gel mixture was relatively high. More specifically, the Cs silicate LDS-1 was easily obtained by heating a silica gel with tetrabutylammonium (TBA) and Cs^+ cations (Si : TBA : Cs = 1 : (0.5–0.75) : (0.5–1)) at 170 °C in an autoclave. In particular, a silica sol was initially prepared by hydrolyzing tetraethoxysilane (25.8 g, 0.124 mol) in ethanol (220 ml) at an ambient temperature with a mixture of water (4.7 g, 0.261 mol) and 60% HNO_3 (3.6 g, 0.034 mol). Then, an ethanol-diluted solution of the silica sol (118 ml) was mixed with 10% TBAOH (129.2 ml, 0.050 mol) aqueous solution and Cs_2CO_3 powder (10.8 g, 0.033 mol). The mixture was evaporated to dryness at 70−90 °C, which resulted in a silica gel that contained TBA and Cs^+ cations. Heating the gel in an autoclave at 170 °C for 5–20 h, which was washed with deionized water and ethanol and dried in air, ultimately yielded the final product. Crystallization times of LDS-1 under both the synthesis conditions were very short as compared to that of $CsHSi_2O_5$ obtained by hydrothermal synthesis (21 days). Additionally, heating up to 500 °C for 24 h using a muffle furnace at an airflow of 1.8 L min^{-1} resulted in calcined LDS-1.

2.2 Physicochemical analysis

The scanning electron micrographs (SEM) were obtained by using a HITACHI S-4800 microscope. The chemical contents in LDS-1 were analyzed by ion-coupled plasma atomic emission spectrometry using a SII SPS-1500R spectrometer. Thermogravimetric analysis was carried out on a MAC Science TG-DTA 2100SA in dried air and the temperature was increased at a rate of 10 K min^{-1}.

Conventional X-ray powder diffraction data for both the as-made and calcined samples were collected on a MAC Science M21X using a flat specimen and Cu-Kα radiation. A solid-state ^{29}Si MAS NMR spectrum was measured at a spinning frequency of 4 kHz using a 4-mm MAS probe, 90° pulse length of 4 μs, and a cycle delay time of 300 s on a Bruker AMX-500 spectrometer operated at 99.65 MHz. The spectra obtained from 1024 scans were accumulated and the ^{29}Si chemical shifts were calibrated using a standard sample of tetramethylsilane. A solid-state ^1H–^{13}C CP/MAS NMR spectrum was also measured at a spinning frequency of 4 kHz and a cycle delay time of 10 s on the same spectrometer operated at 125.78 MHz. The ^1H–^{29}Si CP/MAS and ^1H MAS NMR spectra operated at 400.13 MHz (for ^1H) and 79.495 MHz (for ^{29}Si), respectively, were collected at a spinning frequency of 7 kHz using a 7-mm MAS probe on a Bruker AVANCE 400 WB spectrometer. Additionally, ^{133}Cs MAS NMR spectrum operated at 52.482 MHz was also measured at a spinning frequency of 16 kHz, 90° pulse length of ~2.5 μs, and cycle delay time of 10 s on the latter spectrometer using a 4-mm MAS probe. The ^1H chemical shifts were referenced to tetramethylsilane. The ^{133}Cs chemical shifts were referenced to 1 M CsCl (aq.) *via* a secondary reference of CsCl (solid) at 223.3 ppm. In a sample prepared with TBA, no signal was observed in the ^1H–^{13}C CP/MAS NMR spectra.

2.3 Synchrotron powder diffraction

In order to investigate the detailed crystal structure of LDS-1, the synchrotron X-ray powder diffraction data was collected by using a multiple detector system with six detector arms (Photon Factory BL-4B$_2$).[26] The instrumental geometry was set to the Debye–Scherrer mode. The powder sample was sealed in a glass capillary tube with an inner diameter of 0.5 mm. The sample was spun during measurements in order to improve the randomization of the crystallites. A flat Ge(111) crystal analyzer was mounted at the end of each detector arm with a NaI scintillation counter. The incoming beam was monitored using an ion chamber to account for the decay of the primary beam. The beamline was set up to deliver a relatively short wavelength (λ = 0.70696 Å) in order to decrease absorption correction due to the large amount of Cs^+ cations in the LDS-1 structure.

3. Results and discussion

3.1 Synthesis and physicochemical analysis

The SEM images (Fig. 1) show that LDS-1 is composed of a thin crystalline fibres of approx. 1 × 30 μm in contrast to the crystal morphology of $CsHSi_2O_5$, which has a needle-like shape with a larger crystal size, as shown in ref. 18. LDS-1 is composed of 20.3 wt% Si and 49.1 wt% Cs, yielding a calculated Si/Cs ratio of *ca.* 0.5. LDS-1 was also synthesized without TBAOH. In this case, distilled water was replaced by alkaline electrolytic water with a pH of 11.4 produced by the electrolysis of aqueous NaCl solution (Hoshizaki Electric Co., Ltd.).

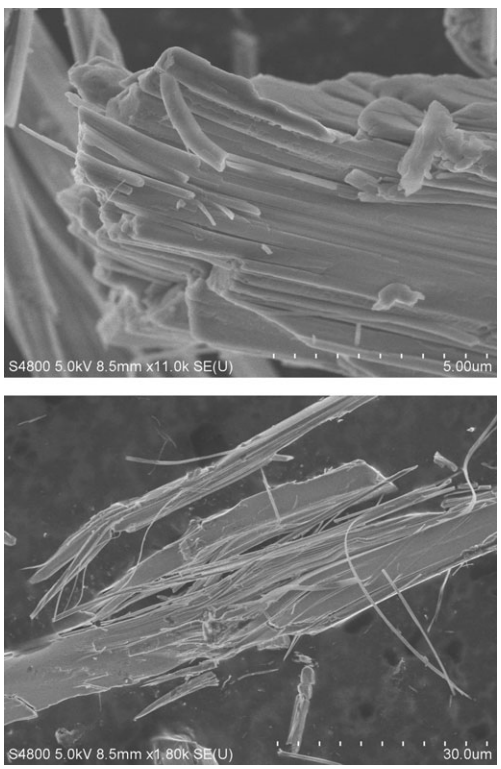

Fig. 1 SEM images of caesium silicate LDS-1.

The same product, LDS-1, was also obtained by heating the gel without TBAOH in the presence of a small amount of water, which was separately placed in the autoclave. Therefore, it is suggested that the role of TBA is to control the pH and to maintain the alkalinity. The higher basicity of the TBA cation seemed effective in the formation of LDS-1.

A slight weight loss was observed up to 400 °C in the TG-DTA data in Fig. 2. In this region, a small amount of adsorbed water, which was estimated to be *ca.* 1.0 wt%, was desorbed. The DTA curve did not show exothermic peaks up to 500 °C (weight loss of *ca.* 3%) and an endothermal peak in a temperature range from 410 to 500 °C. Consequently, it was considered that no partial dehydration condensation of the silicate occurred. The XRD data showed that the as-made LDS-1 exhibited high crystallinity (Fig. 3(a)). LDS-1 changed into a completely different structure after calcination (Fig. 3(b)), although its crystallinity was remarkably degraded. Upon heating above 600 °C, crystalline LDS-1 gradually changed into an amorphous state.

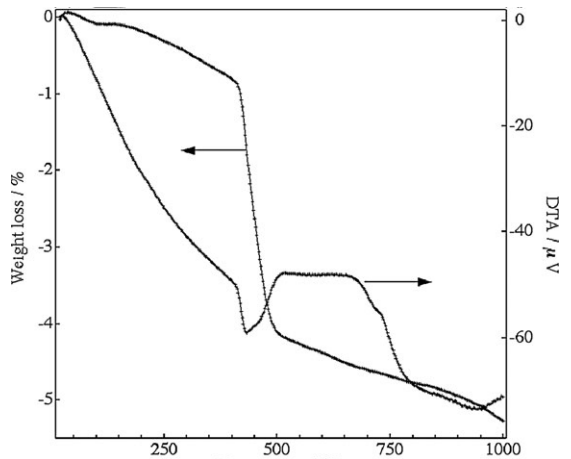

Fig. 2 Thermogravimetric and differential thermal analyses of LDS-1 in air.

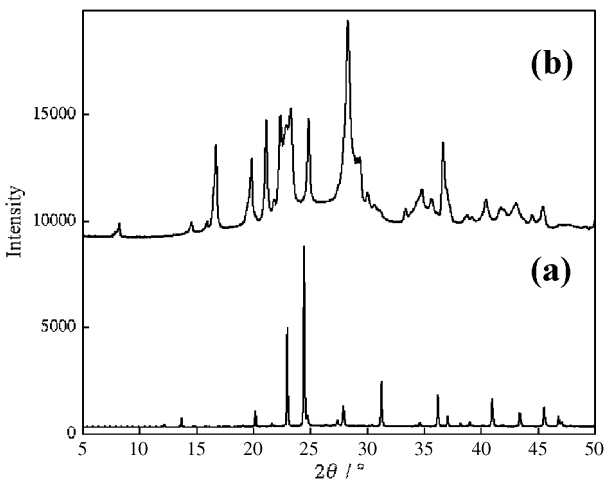

Fig. 3 XRD Patterns for (a) as-made LDS-1 and (b) calcined LDS-1.

3.2 Solid-state NMR

The ^{29}Si MAS NMR spectrum for as-made LDS-1 only showed a sharp singlet at $\delta = -95.4$ ppm (Fig. 4). This peak was assigned to Q^3 silicon atom coordination, *i.e.*, $(SiO)_3SiOH$.[27,28] The ^{1}H–^{29}Si CP/MAS NMR spectra showed a broad peak at *ca.* −94.7 ppm, which indicated that the local structure around the Si atoms was basically attributed to the Q^3 structure. However, strictly speaking, peak splitting of the broad signal was observed. Therefore, several Q^3 peaks that were based on the slightly different local structure around the Si atoms were included in the broad signal. This reveals that the terminal silanols (Si–OH) might be affected by strong interactions from the protons.

In Fig. 5, the ^{1}H MAS NMR spectrum shows a signal derived from strong hydrogen bonding. A very strong high-field peak at a δ value of *ca.* 16.4 ppm was observed, which is due to the strong hydrogen bonding of silanol groups with

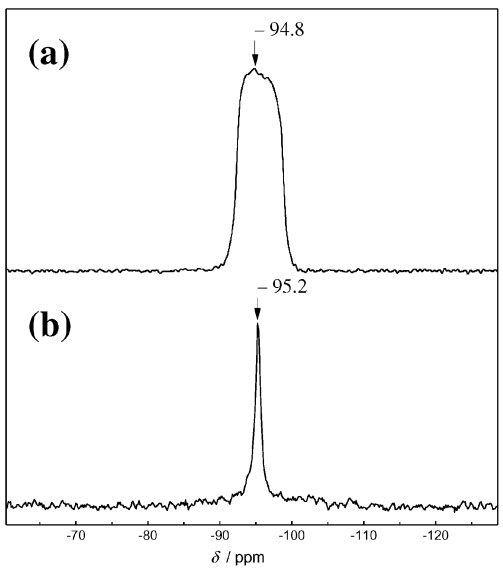

Fig. 4 (a) ^{29}Si MAS NMR and (b) ^{1}H–^{29}Si CP/MAS NMR spectra of LDS-1.

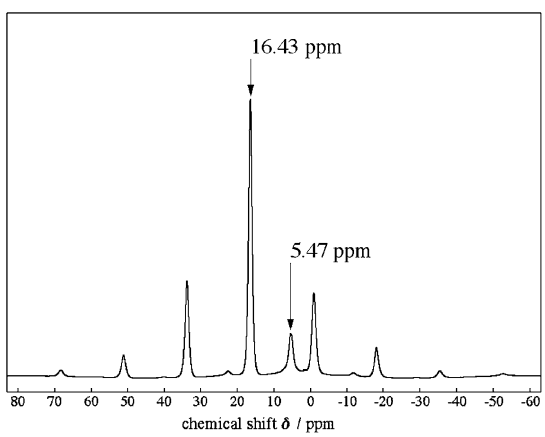

Fig. 5 ^{1}H MAS NMR spectrum of LDS-1. Asterisks and filled squares indicate the spinning sidebands for the low field peak at $\delta = 16.43$ ppm and the high field one at $\delta = 5.47$ ppm, respectively.

d(O–O) = 2.45 Å of the SiO–H···OSi configuration.[22,29–31] The high-field shift can be explained by the following equation: δ/ppm = 79.05 − 0.255d(O–H···O)/pm (picometers). The low-field signal at a δ value of *ca.* 5.4 ppm corresponded to the remaining hydrous species, as described in ref. 28. Furthermore, the obtained ^{133}Cs MAS NMR spectrum exhibited a sharp symmetrical resonance at 51.8 ppm, as shown in Fig. 6, assuming that all the Cs cations are subjected to the same local structure conditions. This value is higher than that of the Cs cation in the cages of several zeolites,[32,33] but it is similar to that of the outer surface of clay minerals, *e.g.*, illite or kaolinite.[34] This finding suggests that the Cs^+ cation is located at some distance from the anionic frameworks and is affected by weak electrostatic potential between the Cs^+ cations and anionic frameworks.

Meanwhile, both ^{29}Si MAS NMR and ^{1}H–^{29}Si CP/MAS NMR spectra of calcined LDS-1 showed a very broad peak at δ values of *ca.* −97.0 ppm and −95.4 ppm, respectively, as shown in Fig. 7. A large intensity of the Q^3 peak was observed in calcined LDS-1, although the local structure around Si atoms might be distorted. Several different Q^2-, Q^3-, and Q^4-type local structures were convoluted into the broad signal.

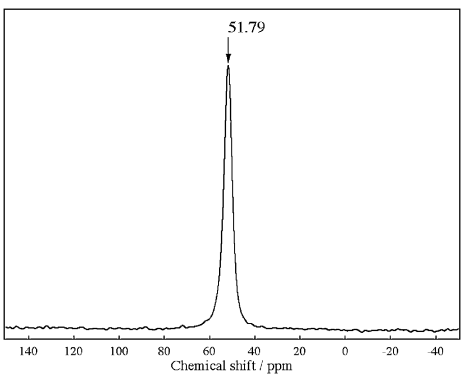

Fig. 6 ^{133}Cs MAS NMR spectrum of LDS-1.

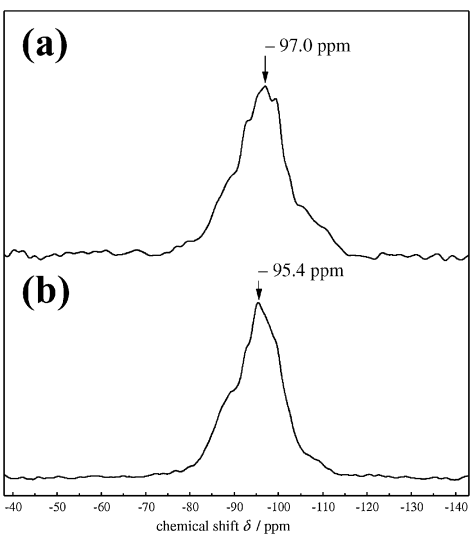

Fig. 7 (a) ^{29}Si MAS NMR and (b) ^{1}H–^{29}Si CP/MAS NMR spectra of calcined LDS-1.

A shoulder peak attributed to the Q^4 structure around a δ value of *ca.* −110 ppm in Fig. 7(a) indicates that some of the Q^3 structures of the Si atoms transformed into the Q^4 structure by dehydration condensation.

3.3 X-Ray structure analysis

The diffraction data was analyzed by the Le Bail,[35] Rietveld, and MPF (MEM-based pattern fitting)[36] methods using the program RIETAN-2000.[37] The MPF method is a sophisticated structure refinement technique at the electron density level from the X-ray powder diffraction data, which is disclosed elsewhere.[36,38] Initially, the indexing of the reflections with DICVOL91[39] yielded a monoclinic unit cell with a = 13.862(3) Å, b = 8.8141(5) Å, c = 4.9798(3) Å, and β = 111.029(9)° with acceptable figures of merit: F_{40} = 213 and M_{40} = 42. The reflection conditions derived from the indexed reflections were $k = 2n$ for $0k0$. Assuming that LDS-1 was centrosymmetric, the space group was $P2_1/m$ (no. 11, setting 1). This symmetry is different from that of $CsHSi_2O_5$ (orthorhombic), although there is not much difference in the unit cell volume between LDS-1 and $CsHSi_2O_5$.

The observed integrated intensities, $|F_{obs}|^2$, of the 821 reflections in the region of $d > 0.92$ Å were extracted using the Le Bail method built in the RIETAN-2000. Anisotropic line broadening was observed in 12 reflections, which were in the 2θ region lower than 21°. Then, a partial profile relaxation[36] with a modified split pseudo-Voigt function was applied to these reflections, which significantly improved the fits between their observed and calculated intensities. The previously extracted integrated intensities were introduced in the direct method program EXPO2004[40] and a structural model for LDS-1 was readily obtained. Thereafter, Rietveld analysis was used to refine the obtained structural parameters. In the initial refinement of the preliminary structure model, we imposed restraints upon all the Si–O bond lengths l(Si–O):l(Si–O) = 1.60 ± 0.03 Å and the O–Si–O bond angles ϕ(O–Si–O):ϕ(O–Si–O) = 109.47 ± 0.5°.

Covalent bonding between the Si and O atoms and hydrogen bonding between adjacent silanols were estimated from previous works using the MPF method at an electron density level. The electron density distributions were calculated from the observed structure factors, F_{obs}, by MEM using the program PRIMA.[41] The MPF method was superior in estimating the unknown partial structure and interpreting disordered structures. Table 1 summarizes the detailed crystallographic information (R factors and lattice parameters). The crystal structural models and electron density distributions were visualized by the program VESTA.[42]

Direct method analyses easily provided the framework topology and Cs^+ cation positions. The silicate framework was an infinite chain, which consisted of only Q^3 silicone atoms, as seen in the structure drawing of LDS-1 viewed from the [010] direction (Fig. 8). Two Si sites and six O sites formed the basic framework, which included continuous four-membered rings, *i.e.*, a chain-like framework. The Cs1 and Cs2 sites were located in the space between adjacent semicircular silicate rings. In the Rietveld refinements, all the atomic displacement parameters, B, for the Si sites were constrained to be equal: B(Si1) = B(Si2). Simple approximations

Table 1 Conditions of the synchrotron XRD experiment and the crystallographic data for caesium chain framework silicate

Compound name	LDS-1
Chemical formula	$Cs_4[Si_8O_{20}H_4]$
M_r	1076.37
Space group	$P2_1/m$ (No. 11)
a/Å	13.8610(3)
b/Å	8.81093(8)
c/Å	4.9785(2)
β/°	111.053(2)
Unit-cell volume, V/Å^3	567.43(2)
Wavelength, λ/Å	0.70696(2)
2θ range/°	5.0–45.0
Step size (2θ)/°	0.006
Counting time per step/s	7
Profile range in FWHM	14
FWHM/° (at 2θ = 10.473°)	0.0345
Number of observations	6669
Number of contributing reflections	821
Number of refined structural parameters	34
Number of background coefficients	12
R_F (Rietveld)	0.0115
R_{wp} (Rietveld)	0.0470
R_e (Rietveld)	0.0335

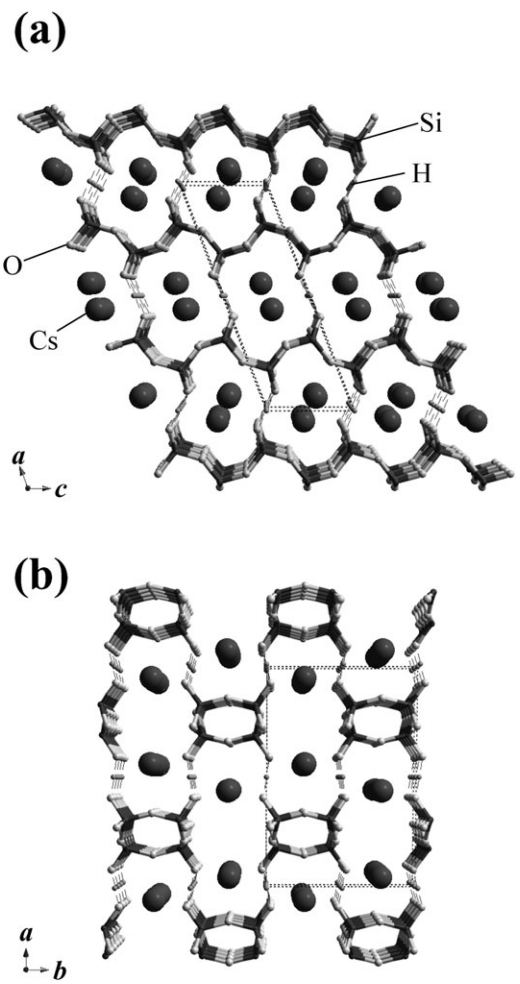

Fig. 8 Structure drawings of LDS-1 viewed from (a) [010] and (b) [001] directions.

B(O1) = B(On: n = 2–6) and B(Cs1) = B(Cs2) were also imposed on the B parameters of the O and Cs sites, respectively. The refined B(Cs) value was relatively large as compared to other B(Si) and B(O) values, indicating that the distribution of the Cs^+ cation was relatively disordered.

Table 2 Structural parameters of LDS-1 obtained by the Rietveld refinements

Atom	Site	g	x	y	z	B/Å^2
Si1	4f	1.0	0.3172(9)	0.4291(15)	0.844(3)	1.19(4)
Si2	4f	1.0	0.1823(9)	0.4276(15)	0.212(3)	= B(Si1)
O1	4f	1.0	0.0849(15)	0.521(3)	0.192(5)	1.76(6)
O2	4f	1.0	0.222(2)	0.464(3)	–0.053(5)	= B(O1)
O3	2e	1.0	0.158(2)	1/4	0.211(7)	= B(O1)
O4	4f	1.0	0.278(2)	0.469(3)	0.506(6)	= B(O1)
O5	2e	1.0	0.345(2)	1/4	0.898(7)	= B(O1)
O6	4f	1.0	0.4150(15)	0.524(3)	0.019(5)	= B(O1)
Cs1	2e	1.0	0.4407(3)	3/4	0.5083(10)	2.34(9)
Cs2	2e	1.0	–0.0555(3)	1/4	0.3780(10)	2.60(3)
H1	2a	1.0	0	0	0	= 3.0[a]
H2	2b	1.0	1/2	0	0	= 3.0[a]

[a] These parameters were fixed to 3 Å^2.

To maintain charge balance, the protons of the silanol groups were positioned between adjacent O6 and O1 sites. Two proton sites were fixed at (0, 0, 0) for site H1 and (1/2, 0, 0) for site H2 since the positions were conveniently given as the weighted centers of the hydrogen bonding as compared to the MEM electron density images (described below). Table 3 shows the geometrical parameters calculated from the refined structural and lattice parameters. The average bond length and bond angle, which are calculated from the lattice and structural parameters, were close to the expected values; these values are in the ranges from 1.55 to 1.63 Å and from 106.5 to 112.5°, respectively. The bond between the Si atom and non-bridging O atom is short (Si2–O1: 1.55 Å). Structural distortion of the framework depended on the charge balance among the open framework, Cs^+ ions, and protons. Dörsam *et al.*[19] also reported this unusually short bond length due to

Table 3 Selected geometric parameters for the LDS-1

	l/Å		ϕ/°
Si1–O2	1.61(3)	O6–Si1–O5	108.5(15)
Si1–O4	1.61(3)	O6–Si1–O4	111.8(17)
Si1–O5	1.629(15)	O6–Si1–O2	111.6(16)
Si1–O6	1.56(2)	O5–Si1–O4	110.8(19)
Si2–O1	1.55(2)	O5–Si1–O2	107.6(17)
Si2–O2	1.63(3)	O4–Si1–O2	106.5(17)
Si2–O3	1.602(15)	O1–Si2–O2	112.5(17)
Si2–O4	1.62(3)	O1–Si2–O3	109.6(15)
		O1–Si2–O4	110.3(16)
Average l	1.60	O2–Si2–O3	108.9(17)
		O2–Si2–O4	106.5(18)
		O3–Si2–O4	109.1(17)
Cs1–O4	3.35(3)		
Cs1–O6	3.07(3)	Average ϕ	109.47
Cs1–O6^{i}	3.35(2)		
Cs1–O6^{ii}	3.46(2)		
Cs2–O1^{iii}	3.07(3)		
Cs2–O1^{iv}	3.39(3)		
Cs2–O1	3.41(2)		
Cs2–O2^{iv}	3.41(3)		
Cs2–O3	3.34(3)		

Symmetry codes: (i) x, y, z + 1; (ii) $-x$ + 1, y + 1/2, $-z$ + 1; (iii) $-x$, y − 1/2, $-z$ + 1; (iv) $-x$, y − 1/2, $-z$.

tetrahedra distortion for $CsHSi_2O_5$. The nearest atomic distance between adjacent silanol groups was short, that is, *l*(O–O) was only *ca.* 2.46 Å for both *l*(O1–O1) and *l*(O6–O6). This fact is in good agreement with the obtained ^{1}H MAS NMR spectra.

In our data, the Rietveld refinement based on the Dörsam's model almost converged, but R_{wp} converged to only 6.4% due to the somewhat high symmetry model. However, the unusually short bond distance was determined as 1.54 Å, which was the almost same value as that found for our monoclinic model. This indicates that the symmetry of LDS-1 is slightly lower compared to that of $CsHSi_2O_5$.

3.4 Electron density distribution by MEM analysis

The MEM electron density maps of LDS-1 clearly show that Cs^+ cations are encapsulated in a pseudo-porous structure with covalent and hydrogen bonding, as shown in Fig. 9. The electron density distributions between the adjacent O6 sites along the [001] direction were revealed by the MPF analysis (Fig. 9(a)), which indicated that the H2 site had strong hydrogen bonding to the O6 sites. Fig. 9(b) shows the electron density distribution of LDS-1 along the [010] direction. The electron density derived from hydrogen bonding due to the H1 site was also observed between adjacent O1 sites. However, no localized electron densities for both the proton sites were observed in Fig. 9 since the scattering amplitude of the proton was too weak and their positions were disordered. Recently, Wang *et al.*[43] and Chen *et al.*[44] reported that similar hydrogen bonds were formed between adjacent silica frameworks in a layered silicate $CsHSi_3O_7$ and a uranyl silicate $K_5(UO_2)[Si_4O_{12}(OH)]$, respectively. The electron density distributions of Cs^+ ions were not spherical but anisotropically elongated, suggesting a positional disorder of the Cs^+ ions.

The final MEM analysis after the MPF refinements afforded *R* factors of $R_F = 1.16\%$ and $wR_F = 0.88\%$. The *R* factors after the Rietveld analyses were also sufficiently low (Table 1). Table 2 summarizes the structural parameters obtained for LDS-1 from the Rietveld refinements. Fig. 10 shows the plots of the observed, calculated and difference patterns for the XRD data against 2θ.

Fig. 11 shows a pseudo-micropore with hydrogen bonding at the electron density level, and the Cs^+ ions were surrounded by pseudo-micropores. The effective pore size and maximum window size are estimated to be *ca.* 12.9 × 2.8 × 2.0 Å and 3.4 × 1.7 Å, respectively, as calculated from the obtained structure model. However, the specific surface area observed was very small from the preliminary N_2 and Ar adsorption measurements. This result indicates that the diffusion of small molecules/atoms such as N_2 and Ar into the pseudo-micropores of LDS-1 might be blocked by Cs^+ cations. Furthermore, the structural model of LDS-1 suggests that the structural transformation from LDS-1 to a microporous structure is difficult by simple calcination due to the insufficient number of protons between the terminal silanols. In order to connect the neighboring silanols by dehydration condensation, the reaction conditions, the following reaction should occur: Si–OH + HO–Si → Si–O–Si + H_2O. Therefore, additional protons are absolutely imperative for condensation by acid treatments or other preparations. Actually, ^{29}Si MAS NMR spectra of the calcined LDS-1 exhibit a large number of Q^3 resonance peaks (Fig. 7), indicating that the dehydration condensation occurred incompletely.

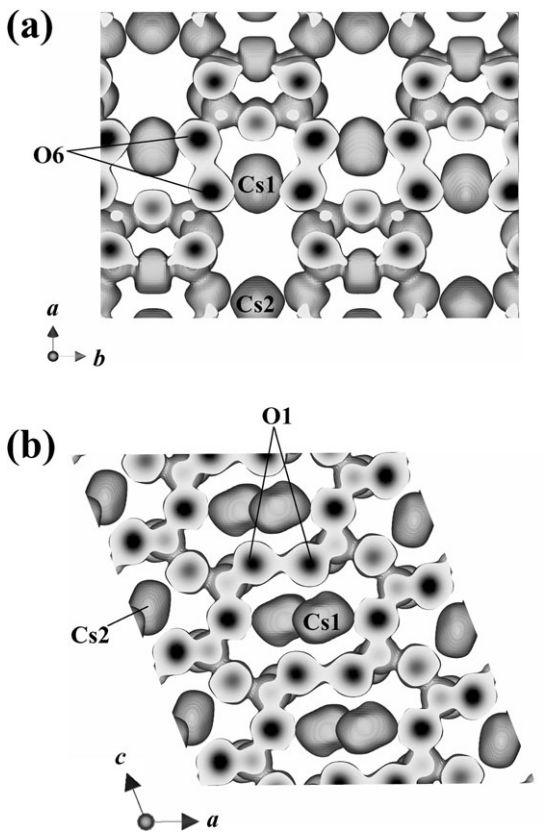

Fig. 9 Structural elucidation for hydrogen bonding between neighboring frameworks in the LDS-1. Electron density distribution images along (a) [001] and (b) [010] directions with equi-surface level of 0.47 e Å^{-3} obtained by the MPF analyses.

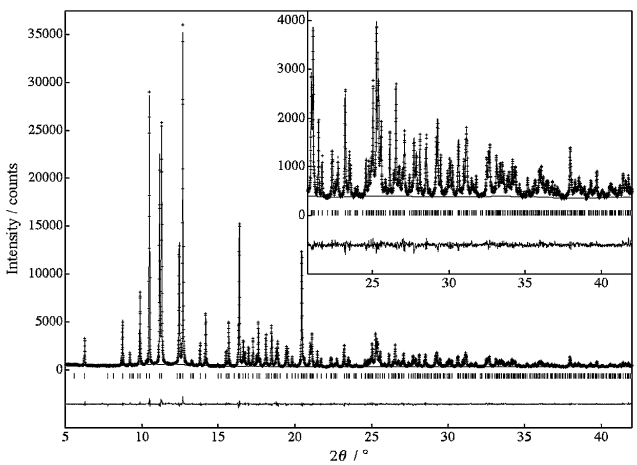

Fig. 10 Observed (crosses), calculated (solid line), and difference patterns obtained by the final MPF structure refinement from the synchrotron XRD data for LDS-1. Tick marks denote the peak positions of possible Bragg reflections.

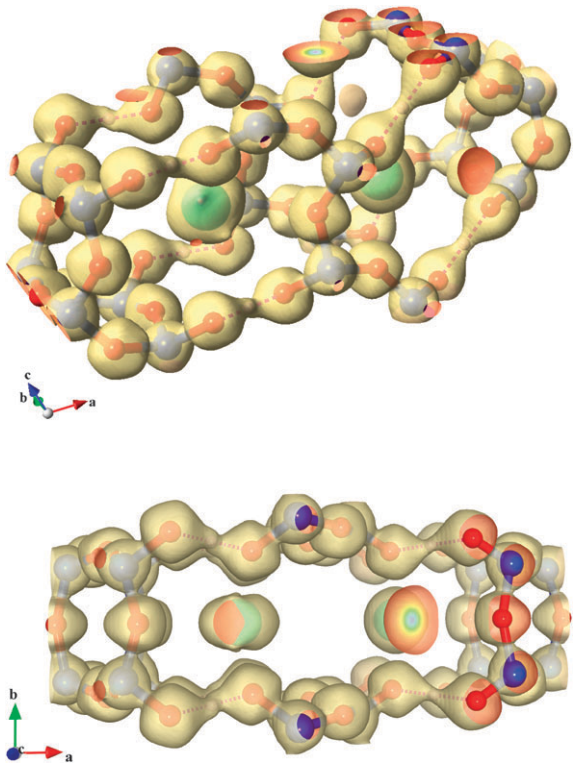

Fig. 11 Electron density 3D images of the pesudo-micropore in LDS-1 along (a) [13$\bar{3}$] and (b) [001] direction. Isosurface level is set to 0.7 e Å^{-3}.

4. Conclusions

The crystal structure of the low-dimensional caesium silicate, LDS-1, was determined by *ab initio* structure analyses using high-resolution synchrotron powder diffraction data. LDS-1 is composed of one-dimensional zigzagged frameworks, where the Cs ions are wedged between the frameworks. Our structural model is in good agreement with Dörsam's model, although the crystal symmetries are different between the two models. Adjacent silanol groups are interconnected by strong hydrogen bonding with a bond distance between neighboring O atoms of 2.45 Å, which are observed in the electron density distribution by MPF refinement. The results of solid-state MAS NMR measurements strongly support the obtained structural features. The electron density images also show pseudo-micropores formed between adjacent zigzagged frameworks with strong hydrogen bonding and Cs^+ cations enclosed by pseudo-micropores. These facts imply that LDS-1 can transform into the microporous structure with the topology of zeolite ABW by dehydration condensation after chemical treatments. The crystallinity of LDS-1 is severely degraded by calcination in air. The XRD pattern of calcined LDS-1 also shows that a novel compound is formed, whose structure is unresolved at the present time. Currently, we are examining the conversion from LDS-1 to microporous structures by means of various sample treatments.

Acknowledgements

The author thanks Prof. Ida (Nagoya Institute of Technology) for his support of the synchrotron experiment. This work was supported by a Grant-in-Aid for Scientific Research (20310066) from MEXT, Japan, to T. I. The synchrotron experiment was conducted with the approval of the Photon Factory of KEK (Proposal No. 2000P012).

References

1 R. M. Barrer, in *Zeolites and Clay Minerals as Sorbents and Molecular Sieves*, Academic Press, New York, 1978.
2 S. Shimizu, Y. Kiyozumi, K. Maeda, F. Mizukami, G. Pál-Borbély, R. M. Mihályi and H. K. Beyer, *Adv. Mater.*, 1996, **8**, 759.
3 G. Pál-Borbély, H. K. Beyer, Y. Kiyozumi and F. Mizukami, *Microporous Mesoporous Mater.*, 1998, **22**, 57.
4 M. Salou, Y. Kiyozumi, F. Mizukami, P. Nair, K. Maeda and S. Niwa, *J. Mater. Chem.*, 1998, **8**, 2125.
5 M. Salou, Y. Kiyozumi, F. Mizukami and F. Kooli, *J. Mater. Chem.*, 2000, **10**, 2587.
6 M. Salou, F. Kooli, Y. Kiyozumi and F. Mizukami, *J. Mater. Chem.*, 2001, **11**, 1476.
7 Y. Kiyozumi, F. Mizukami, Y. Akiyama, T. Ikeda and T. Nishide, *Stud. Surf. Sci. Catal.*, 2001, **135**, 191.
8 F. A. Cotton and G. Wilkinson, in *Advanced Inorganic Chemistry*, Wiley-Interscience, New York, 5th edn, 1988.
9 B. E. Warren, *Z. Kristallogr. Kristallgeom. Kristallphys. Kristallchem.*, 1930, **72**, 493.
10 J. A. Gard and H. F. W. Taylor, *Acta Crystallogr.*, 1960, **13**, 785.
11 W. S. McDonald and D. W. J. Cruickshank, *Acta Crystallogr.*, 1967, **22**, 37.
12 J. R. Clark, D. E. Appleman and J. Papike, *J. Am. Mineral.*, 1973, **58**, 594.
13 H. P. Grosse and E. Tillmanns, *Cryst. Struct. Commun.*, 1974, **3**, 603.
14 K. F. Hesse, *Acta Crystallogr., Sect. B*, 1973, **33**, 901.
15 T. Murakami, Y. Takeuchi and T. Yamanaka, *Z. Kristallogr.*, 1984, **166**, 263.
16 G. Y. Chao, *Can. Mineral.*, 1986, **24**, 417.
17 R. M. Wentzcovitch, D. A. Hugh-Jones, R. J. Angel and G. D. Price, *Phys. Chem. Miner.*, 1995, **22**, 453.
18 *Jpn. Pat.*, 289 725, 2005.
19 G. Dörsam, V. Kahlenberg and R. X. Fischer, *Z. Anorg. Allg. Chem.*, 2003, **629**, 981.
20 T. Ikeda, Y. Oumi, Y. Akiyama, A. Kawai and F. Mizukami, *Angew. Chem., Int. Ed.*, 2004, **43**, 4892.
21 S. Zanardi, A. Alberti, G. Cruciani, A. Corma, V. Fornés and M. Brunelli, *Angew. Chem., Int. Ed.*, 2004, **43**, 4933.
22 Y. X. Wang, H. Gies, B. Marler and U. Müller, *Chem. Mater.*, 2005, **17**, 43.
23 B. Marler, N. Ströter and H. Gies, *Microporous Mesoporous Mater.*, 2005, **83**, 201.
24 M. Sakata and M. Sato, *Acta Crystallogr., Sect. A*, 1990, **46**, 263.
25 S. Shimizu, Y. Kiyozumi and F. Mizukami, *Chem. Lett.*, 1996, 403.
26 H. Toraya, H. Hibino and K. Ohsumi, *J. Synchrotron Radiat.*, 1996, **3**, 75.
27 M. Mägi, E. Lippmaa, A. Samoson, G. Engelhardt and A. R. Grimmer, *J. Phys. Chem.*, 1984, **88**, 1518.
28 G. Engelhardt and D. Michel, in *High-Resolution Solid-state NMR of Silicates and Zeolites*, Wiley, Chichester, 1987.
29 H. Eckert, J. P. Yesinowski, L. A. Silver and E. M. Stolper, *J. Phys. Chem.*, 1988, **92**, 2055.
30 C. Gardiennet and P. Tekely, *J. Phys. Chem. B*, 2002, **106**, 8928.
31 D. F. Shantz and R. F. Lobo, *Chem. Mater.*, 1998, **10**, 4015.
32 M. K. Ahn and L. E. Iton, *J. Phys. Chem.*, 1995, **95**, 4496.
33 A. M. Geoffery, A. Ozin and P. M. Macdonald, *J. Phys. Chem.*, 1996, **100**, 16662.
34 Y. Kim and R. J. Kirkpatrick, *Geochim. Cosmochim. Acta*, 1997, **61**, 5199.
35 A. Le Bail, H. Duroy and J. L. Fourquet, *Mater. Res. Bull.*, 1988, **23**, 447.
36 F. Izumi, S. Kumazawa, T. Ikeda and T. Ida, *Powder Diffraction*, ed. S. P. Sen Gupta, Allied Publishers, New Delhi, 1998, ch. 2.
37 F. Izumi and T. Ikeda, *Mater. Sci. Forum*, 2000, **321–324**, 198.

38 T. Ikeda, T. Kodaira, F. Izumi, T. Ikeshouji and K. Oikawa, *J. Chem. Phys. B*, 2004, **108**, 17709.
39 A. Boultif and D. Louer, *J. Appl. Crystallogr.*, 1991, **24**, 987.
40 A. Altomare, M. C. Burla, M. Camalli, B. Carrozzini, G. L. Cascarano, C. Giacovazzo, A. Guagliardi, A. G. G. Moliterni, G. Polidori and R. Rizzi, *J. Appl. Crystallogr.*, 1999, **32**, 339.
41 F. Izumi and R. A. Dilanian, *Recent Research Developments in Physics*, Transworld Research Network, Trivandrum, 2002, vol. 3, Part II, pp. 699–726.
42 F. Izumi and K. Momma, *Solid State Phenom.*, 2007, **130**, 15.
43 X. Wang, L. Liu, J. Huang and A. J. Jacobson, *J. Solid State Chem.*, 2004, **177**, 2499.
44 C. Chen, H. Kao and K. Li, *Inorg. Chem.*, 2005, **44**, 935.